Benzo[a]pyrene induces oxidative stress and endothelial progenitor cell dysfunction via the activation of the NF-κB pathway

KANGTING JI[1], CHENG XING[1], FENGCHUN JIANG[1], XIAOYAN WANG[1], HUIHUI GUO[1], JINLIANG NAN[1], LU QIAN[1], PENGLIN YANG[1], JIAFENG LIN[1], MEIDE LI[2], JINNONG LI[2], LIANMING LIAO[2] and JIFEI TANG[1]

[1]Department of Cardiology, The Second Affiliated Hospital, Wenzhou Medical College, Wenzhou, Zhejiang; [2]Academy of Integrative Medicine, Fujian University of Traditional Chinese Medicine, Fuzhou, Fujian, P.R. China

Received December 8, 2012; Accepted February 8, 2013

DOI: 10.3892/ijmm.2013.1288

Abstract. Smoking is a major risk factor for atherosclerosis. In this study, we evaluated the effects of benzo[a]pyrene (BaP, a prominent component of tobacco smoke) on the function and pro-inflammatory response of human endothelial progenitor cells (EPCs). EPCs were isolated from umbilical cord blood and treated with different concentrations (10, 20 and 50 μmol/l) of BaP. The proliferation, migration, adhesion and angiogenesis of BaP-treated EPCs were evaluated using the cell counting kit-8 (CCK-8), Transwell assay, adhesion assay and *in vitro* tube formation assay, respectively. The activation of nuclear factor-κB (NF-κB) was evaluated by measuring the mRNA expression of NF-κB p65 and p50 by real-time RT-PCR and NF-κB translocation assay. Reactive oxygen species (ROS) production was determined by the reduction of fluorescent 2',7'-dichlorofluorescein diacetate (DCFH-DA). The results demonstrated that BaP treatment significantly inhibited the proliferation, migration, adhesion and angiogenesis of EPCs *in vitro*. In addition, BaP induced the release of interleukin (IL)-1β and tumor necrosis factor-α from these cells. Moreover, the exposure of EPCs to BaP induced ROS generation and the activation of NF-κB. Experiments with EPCs pre-treated with pyrrolidine dithiocarbamate, an inhibitor of NF-κB, revealed that the BaP-mediated inhibition of proliferation, migration, adhesion and angiogenesis of EPCs is mainly regulated by NF-κB. Thus, tobacco smoke may induce oxidant-mediated stress responses in EPCs and impair their function via the activation of the NF-κB pathway.

Correspondence to: Dr Jifei Tang, Department of Cardiology, The Second Affiliated Hospital, Wenzhou Medical College, 109 Xueyuan Road, Wenzhou, Zhejiang 325027, P.R. China
E-mail: jefftang@medmail.com.cn

Dr Lianming Liao, Academy of Integrative Medicine, Fujian University of Traditional Chinese Medicine, 1 Huatuo Road, Fuzhou, Fujian 350122, P.R. China
E-mail: llm@fjtcm.edu.cn

Key words: smoking, atherosclerosis, benzo[a]pyrene, endothelial progenitor cell, nuclear factor-κB, reactive oxygen species

Introduction

Cigarettes are possibly the single most significant source of toxic chemical exposure and chemically-mediated illness in humans. The World Health Organization forecasts that cigarettes will kill approximately 10 million individuals per year globally by the year 2020 (1). Indeed, tobacco-assoicated cancers account for a considerable proportion of cancer-related deaths. In addition, cigarette smoking is a powerful risk factor for atherosclerotic cardiovascular disease and is associated with the increased incidence of stroke and coronary artery disease (2-4). Among the toxic compounds contained in tobacco smoke are polycyclic aromatic hydrocarbons (PAHs), such as benzo[a]pyrene (BaP) (5). BaP is readily absorbed following inhalation and is rapidly distributed to several tissues, including the kidneys, small intestine, trachea, stomach, testes, liver and oesophagus. BaP is metabolised by cytochrome P450 enzymes, resulting in the formation of a number of metabolites, including the reactive epoxide metabolite, BaP 7,8-diol-9,10-epoxide, which may bind to DNA and is believed to be responsible for its carcinogenicity (6). In addition, BaP may impair lysosomes and break down cellular membranes (7).

There is strong evidence to suggest oxidative stress is one of the most potent inductors of vascular inflammation in atherogenesis (8,9). Reactive oxygen species (ROS) are known to change the oxidation-reduction (redox) state of exposed cells, and it is known that several inflammatory genes and the related transcription factors are regulated through redox-sensitive mechanisms (10). Nuclear factor-κB (NF-κB) may respond directly to oxidative stress and the activation of NF-κB is a key redox-sensitive event associated with vascular dysfunction. Endothelial dysfunction is an early hallmark of atherosclerosis. Endothelial progenitor cells (EPCs) play an important role in restoring vascular tone in response to vascular injury. Mature endothelial cells have a very low regenerative capacity, compared with circulating EPCs, which can proliferate, migrate and differentiate into mature endothelial cells (11-13). EPCs have been shown to enhance the formation of new endothelium in animal models, in which vessel injury occurs after balloon injury, myocardial infarction, or heart transplantation (14). Thus, the presence of healthy EPCs is crucial to post-event vascular reconstruction (15).

In animal models, BaP alone has been shown to induce atherosclerotic lesions (16,17), and repeated cycles of vascular injury by BaP increase the onset and progression of atherosclerotic lesions in animals. This atherogenic response is partly mediated by the activation of cis-acting antioxidant/electrophile response elements that enhance c-Ha-ras transcription in vascular smooth muscle cells. The activation of antioxidant/electrophile responsive cis-acting elements may depend on the metabolism of BaP by cytochrome P450 enzymes to intermediates that induce oxidative stress and modulate gene expression. It remains unclear whether BaP affects the function of EPCs. Since BaP has been implicated in the initiation and progression of atherosclerotic vascular lesions and EPCs have been implicated in the repair of vascular lesions, in this study, we investigated the effects of BaP on the function of EPCs. We also evaluated the role of redox mechanisms and NF-κB modulation during this process.

Materials and methods

Reagents. BaP was purchased from Sigma (St. Louis, MO, USA). For the fluorescence-activated cell sorter (FACS) analyses, the mouse IgG antibodies (FITC, perCP, and PE) and anti-human CD34-PE antibody were from Caltag Laboratories. The anti-human VE-Cadherin-FITC antibody was from Bender MedSystem™ Austria. The anti-human VEGFR-2-PE and AC133-FITC antibodies were from R&D System. The Cell Counting Kit-8 (CCK-8) was obtained from Dojindo Laboratories (Kumamoto, Japan).

Cells and culture conditions. Informed consent was obtained from all participating mothers. The study was approved by the Institutional Review Board of the Second Affiliated Hospital, Wenzhou Medical College, Wenzhou, China. Umbilical cord blood (~50 ml) from a normal delivery was collected by needle/syringe from the placental side of the umbilical vein after the newborn was delivered but prior to placental delivery. Samples were processed within 2 h, and cord blood mononuclear cells were isolated from umbilical cord blood by Ficoll gradient centrifugation. Cells were seeded at $5x10^6/cm^2$ into 6-well culture dishes which were pre-coated with fibronectin (Roche Applied Science, Indianapolis, IN, USA). The culture medium was endothelial growth medium-2 (EGM-2; Lonza, Basel, Switzerland), which contains fetal calf serum (FCS, 10%, w/v), and antibiotics. Cells were cultured in humidified incubators with 5% CO_2 and initially allowed to adhere for 24 h, followed by medium change every 3 days. When cultures reached over 90% confluence, adherent cells were detached with 0.05% trypsin-EDTA (Gibco, Carlsbad, CA, USA) and replated.

Flow cytometry. Second passage cells were collected, washed twice in ice-cold FACS buffer containing phosphate buffer (pH 7.2) with 5 mm EDTA and 5% fetal bovine serum (FBS), and adjusted to $1x10^6$ cells/ml. At least 50,000 cells were incubated with fluorescence-labeled monoclonal antibodies or the respective isotype control (1/20 diluted, 4˚C, 30 min). After the washing steps, the labeled cells were analyzed by flow cytometry using a FACSCalibur flow cytometer and CellQuest Pro software (BD Biosciences, Bedford, MA, USA). In addition, GSC7901 (a gastric cancer cell line) was used as the control.

Immunocytochemistry. After culture for 6 days, adherent cells were incubated with the fluorescent probe 1,1'-dioctadecyl-1-3,3,3',3'-tetramethyl-indo-carbocyanine perchlorate-acetylated-LDL (DiI-Ac-LDL; 2.4 μg/ml; Molecular Probes) or rhodamine conjugated lectin (Lectin Kit; Sigma) at 37˚C for 4 h. After staining, samples were viewed under an inverted fluorescent microscope (Leica, Wetzlar, Germany). Surface binding of rhodamine conjugated lectins was green and ac-LDL in cytoplasm was red.

Factor VIII-related antigen immunohistochemistry. After the cultured cells were fixed with 95% (v/v) alcohol for 30 min, 0.5% (v/v) H_2O_2 methanol was added to inactivate endogenous peroxidase. The cells were then incubated with diluted primary antibody (1:1,000) overnight at 4˚C, followed by incubation with the secondary antibody and strept actividin-biotin complex (SABC) for 20 min in the oven at 37˚C according to standard protocols. Positive cells were stained brown. Gastric cancer cells (GSC7901) acted as the negative control.

Cell proliferation assay. Cell proliferation was quantified using CCK-8. Briefly, cells were plated in flat-bottomed 96-well microplates at $1x10^4$ cells/well and incubated in EGM-2 medium containing 2% carboxyfluorescein (CFS) for 24 h (3 wells/group). The culture medium was then changed to EGM-2 medium containing 10% CFS and cultured for an additional 2 h. Cells were then exposed to BaP at concentrations of 10, 20 and 50 μmol/l for 24 h to examine the effects of BaP. BaP was dissolved in DMSO and diluted to the desired final concentrations in culture medium. The control cells were left untreated and the solvent control cells were incubated with DMSO alone (1 ml/l). CCK-8 (10 μl/well) was added to the wells at the end of the experiment. After incubation at 37˚C for 4 h, the absorbance of each well was determined using a microplate reader at 450 nm. The degree of cell proliferation was determined as the percentage of absorbance of the treated cells to that of the control cells.

Migration assay. After the cells were cultured in the absence or presence of BaP (10, 20 and 50 μmol/l) for 24 h as described above, adhesive cells were digested, collected and resuspended in EBM-2 medium containing 2% FBS and 0.1 bovine serum albumin (BSA). Cells were adjusted to $5x10^5$ cells/ml. Cell migration was quantified by a Transwell chemotaxis assay using a Boyden chamber (18). Briefly, $5x10^4$ cells (100 μl) were plated in the upper of 2 chambers divided by a membrane with 8 μm pores (Transwell; Corning). EBM-2 medium containing 10% FBS (600 μl) was added to the lower chamber. After 24 h, the membranes were washed twice in D-Hank's solution (Gibco) and fixed in 4% formaldehyde. After wiping the cells off the upper side of the membrane with a cotton swab (Q-tip), the membranes were detached and mounted on glass slides with 0.25% crystal violet. Migrated cells were counted under a microscope. Each experimental condition was performed in triplicate, and the number of migrated cells was determined from 10 random x400 high-power fields/membrane.

Cell adhesion assay. After the cells were cultured in the absence or presence of BaP (10, 20 and 50 μmol/l) for 24 h as described above, adhesive cells were digested, collected and resuspended in EGM-2 medium containing 2% FBS.

Cell-matrix adhesion was investigated in 96-well plates coated overnight (4˚C) with fibronectin (1 μg/ml). Cells were seeded at $5x10^3$ cells/well in 100 μl. Adhesion was carried out for 30 min at 37˚C, 5% CO_2. After the removal of non-adherent cells by 2 washing steps with EGM-2 medium containing 2% FBS at room temperature, adhesion was quantified by counting the adherent cells from 10 random x200 high-power fields under an inverted microscope.

Tube formation assay. Matrigel (BD Biosciences) was dissolved at 4˚C overnight, and 96-well plates were prepared with 50 μ Matrigel in each well after coating and incubating at 37˚C for 60 min as previously described (19). After the cells were cultured in the absence or presence of BaP (10, 20 and 50 μmol/l) for 24 h as described above, adhesive cells were digested, collected and resuspended in EGM-2 medium containing 2% FBS and 0.1 BSA. Cells were adjusted to $5x10^5$ cells/ml. EPCs of $1x10^5$ were added to the gel. After 24 h of incubation at 37˚C, the number of tubes formed was determined from 5 random x400 high-power fields under a light microscope.

Measurement of intracellular ROS. The oxidation of 2',7'-dichlorofluorescein diacetate (DCFH-DA; Sigma-Aldrich) to 2',7'-dichlorofluorescein (DCF) was used to estimate ROS levels as previously described (20). Cells at passage 3 were digested, collected and plated in a 6-well plate with EGM-2 medium containing 2% FBS for 24 h. There was a slide pre-coated with fibronectin in each well. The cells ($5x10^6$/ml) were then cultured in the absence or presence of BaP (10, 20 and 50 μmol/l) for an additional 24 h as described above. Thereafter, the cells were incubated with 10 μmol/l chloromethyl-dihydrodichlorofluorescein diacetate (CM-H2DCF-DA) for 3 h at 37˚C. After removal of the medium and washing of the cells twice, the slide was removed and the fluorescence intensity (relative fluorescence units) was measured at an excitation and emission wavelength of 488 and 522 nm, respectively, using a spectrofluorometer (Hitachi). The fluorescence intensity was measured by image analysis Image-Pro Plus 6.0 software.

Measurement of malondialdehyde (MDA) and superoxide dismutase (SOD) in supernatants. MDA in the supernatants was measured using a commercial kit (Jiancheng Bioengineering Co., Ltd., Nanjing, China) according to the manufacturer's instructions that utilizes the measurement of thiobarbituric acid-reactive substances (TBARS).

SOD activity was measured using a superoxide dismutase assay kit (Jiancheng Bioengineering Co., Ltd., Nanjing, China) according to the manufacturer's instructions.

Real-time RT-PCR analysis. Total RNA was isolated and transcribed to cDNA using the RT-PCR kit (MBI Fermentas, Burlington, ON, Canada). RNA (1 μg) was reverse transcribed in a total volume of 20 μl. An aliquot of 1 μl of the reverse transcription reaction was used in the real-time PCR reactions (20 μl final volume) and performed in a LightCycle 480 Thermocycler (Roche). Fold inductions were calculated using the cycle threshold $\Delta\Delta$Ct method as previously described (21,22). Briefly, PCR was performed at 95˚C (30 sec) followed by 40 cycles at 95˚C (5 sec)/60˚C (20 sec). SYBR-Green intercalating dye was used for signal detection. For each sample, the number of cycles required to generate a given threshold signal (Ct) was recorded. With a standard curve generated from serial dilutions of sample cDNA, the ratio of NF-κB p65 or p50 expression relative to GAPDH expression was calculated for each experimental group and normalized relative to an average of ratios from the control group. The sequences of the primers used in this study were as follows: p65 forward, 5'-CACCGGATTGAGGAGAAACGT-3' and reverse primer, 5'-ATCTGCCCAGAAGGAAACACC-3'; p50 forward, 5'-GGATTTCGTTTCCGTTATGTATGT-3' and reverse primer, 5'-TGTCCTTGGGTCCAGCAGTT-3'; and ACTB forward, 5'-CGTGGACATCCGCAAAGAC-3' and reverse primer, 5'-AAGAAAGGGTGTAACGCAACTAAG-3'.

Enzyme-linked immunosorbent assay (ELISA). Cells at passage 3 were digested, collected and plated in EBM-2 medium containing 2% FBS for 24 h. Cells were then cultured in the absence or presence of BaP (10, 20 and 50 μmol/l) for an additional 24 h as described above. Using supernatant samples, ELISA was performed with ELISA kits (Westang Biotechnological Co., Ltd., Shanghai, China) for interleukin (IL)-1β and tumor necrosis factor (TNF)-α, as indicated in the manufacturer's instructions.

NF-κB translocation assay. NF-κB translocation in the cells was examined using a NF-κB activation kit (Beyotime Institute of Biotechnology, Shanghai, China) which contains DAPI, anti-NF-κB p65 monoclonal antibody (mAb) and secondary Cy3-conjugated mAB dyes. Cells at passage 3 were digested, collected and plated in EBM-2 medium containing 2% FBS for 24 h. The cells were then cultured in the absence or presence of BaP (10, 20 and 50 μmol/l) for an additional 24 h as described above. Fixation, permeabilization, and immunofluorescence staining of the cells were performed according to the manufacturer's instructions. The difference between the intensity of nuclear and cytoplasmic NF-κB-associated fluorescence was reported as translocation parameter.

Effect of NF-κB inhibition on BaP-induced EPC dysfunction. To evaluate the role of NF-κB in BaP-induced dysfunction, pyrrolidine dithiocarbamate (PDTC, 25, 50 and 75 μmol/l), an antioxidant that has been shown to selectively inhibit NF-κB activation, was added to the culture 2 h before BaP was added in the above experiments (23).

Statistical analysis. Data are expressed as the means ± standard deviation (SD). Differences between data sets were assessed by one-way ANOVA. A P-value <0.05 was considered to indicate a statistically significant difference.

Results

Characterization of EPCs from human umbilical cord blood. EPCs were isolated from human umbilical cord blood mononuclear cells. At day 4, cell colonies appeared and the colonies had a typical cobblestone shape under a phase-contrast inverted microscope (Fig. 1A). Immunochemistry showed that the cells were positive for factor VIII (Fig. 1B). To confirm that the cells acquired endothelial phenotypes after becoming adherent, fluorescent staining was used to detect double-positive cell binding of FITC-labeled Ulex europaeus

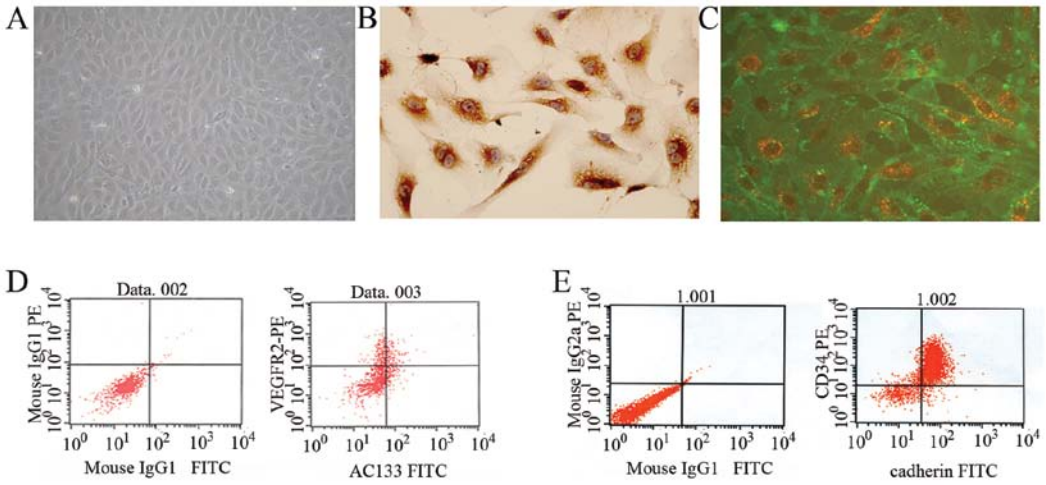

Figure 1. Characterization of endothelial progenitor cells (EPCs). (A) Cells had a typical cobblestone shape as shown by a phase-contrast inverted microscope. (B) Immunochemistry showed that the cells were positive for factor VIII. (C) Fluorescent staining showed that the cells were positive for Ulex europaeus agglutinin-1 (UEA-1) and 1,1'-dioctadecyl-1-3,3,3',3'-tetramethyl-indo-carbocyanine (DiI). (D and E) FACS analysis showed that the cells were positive for VEGFR-2, AC133, CD34 and VE-cadherin.

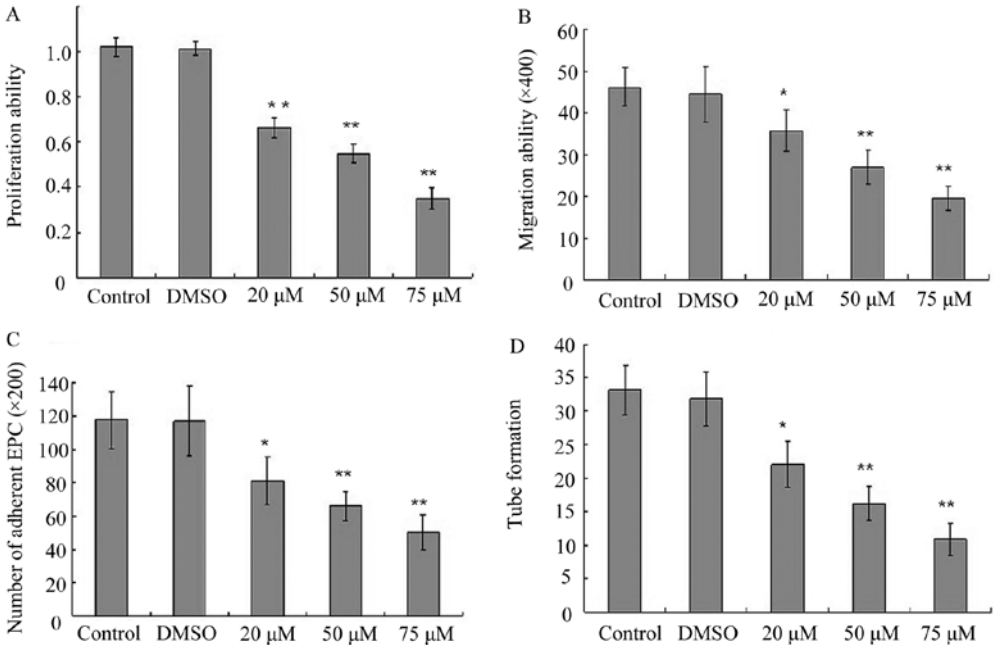

Figure 2. (A) BaP induces endothelial progenitor cell (EPC) dysfunction *in vitro*. EPCs were cultured in the absence (control) or in the presence of 1, 10 and 20 M BaP for 24 h. BaP inhibited the (A) proliferation, (B) migration, (C) adhesion and (D) angiogenesis of EPCs *in vitro*. Data represent the means ± SEM of at least 3 independent experiments. *P<0.05 vs. control; **P<0.01 vs. control.

agglutinin-1 (UEA-1) lectin and DiI-labeled acetylated low-density lipoprotein (Fig. 1C). To further characterize the EPCs, FACS analysis was performed. Immunophenotyping revealed that *ex vivo* expanded EPCs expressed VEGFR-2 (60.95±0.88%), AC133 (16.08±0.44%), CD34 (77.19±3.32%) and VE-cadherin (25.54±0.73%) (Fig. 1D and E). This cell population is consistent with the early pro-angiogenic EPC type described by other authors (24,25).

Effect of BaP on EPC proliferation. In order to investigate the cytotoxic effects of BaP on EPCs, cell proliferation assay was performed. BaP inhibited the cell proliferation in a dose-dependent manner for 24 h (Fig. 2A). Therefore, the concentration of BaP of 20 μM was selected for the experiments.

BaP inhibits migration of EPCs. Considering that the migratory capability of EPCs is crucial for the mobilization of EPCs from the bone marrow into peripheral blood, we then examined the effect of BaP on the migratory capability of EPCs using Transwell assay. BaP significantly reduced the migratory capability of EPCs in a dose-dependent manner (Fig. 2B).

BaP inhibits adhesion of EPCs. Adhesion assays were performed to examine the adhesion of EPCs to fibronectin. The cell-matrix adhesion of EPCs to immobilized fibronection was substantially downregulated by BaP in a dose-dependent manner (Fig. 2C).

BaP inhibits in vitro capillary-like structure formation of EPCs. To examine the effects of BaP on the capacity of EPCs to

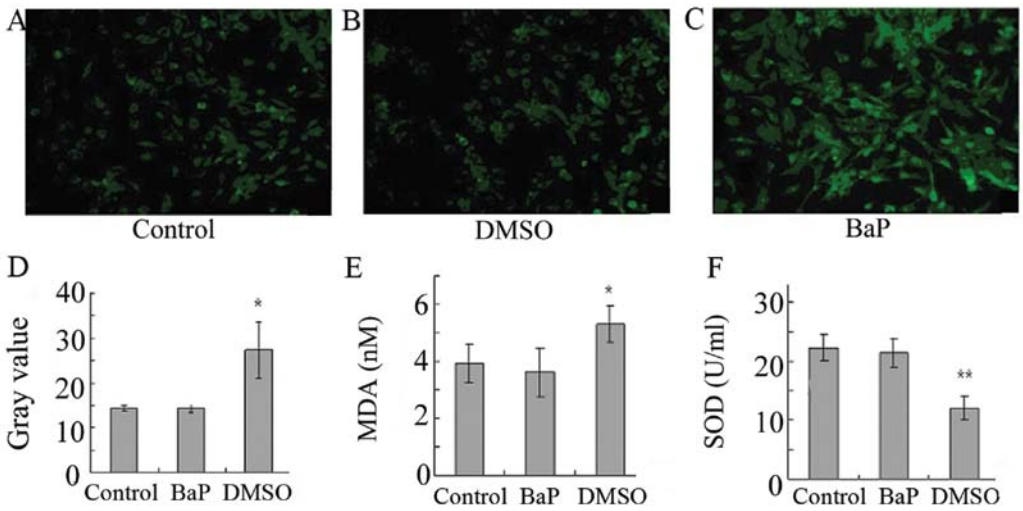

Figure 3. (A-D) BaP increases oxidative stress in endothelial progenitor cells (EPCs). The treatment of EPCs with BaP (20 μM) for 45 min significantly increased cellular ROS levels, as indicated by the gray value of green fluorescence. (E and F) BaP increased the production of malondialdehyde (MDA) and suppressed the production of superoxide dismutase (SOD). These data demonstrate that BaP increases oxidative stress in EPCs. Data represent the means ± SEM of at least 3 independent experiments. *P<0.05 vs. control; **P<0.01 vs. control.

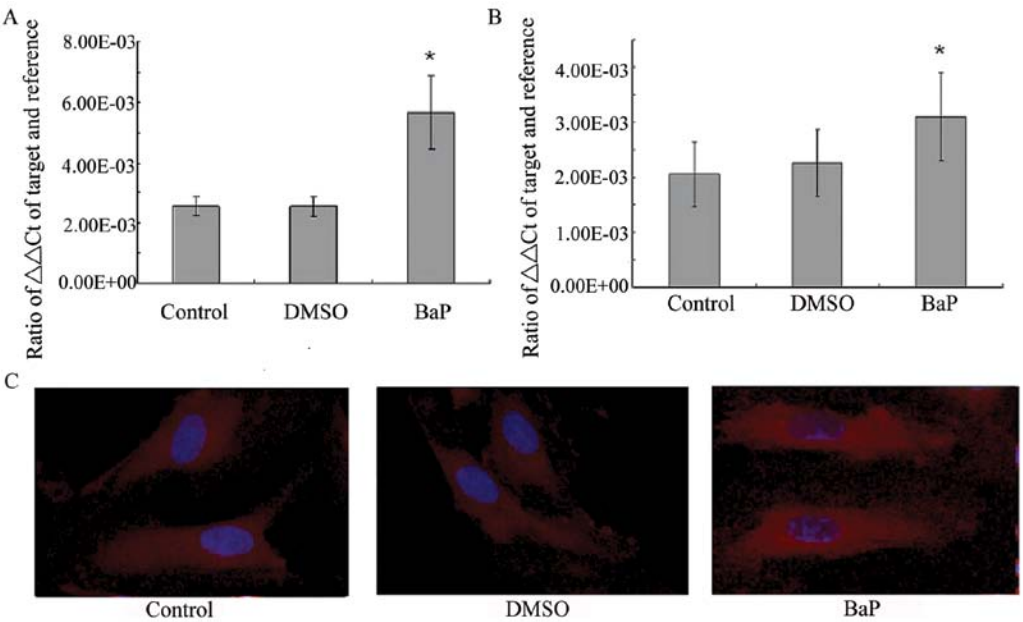

Figure 4. BaP increases NF-κB expression and causes NF-κB p65 translocation. Data represent the means ± SEM of at least 3 independent experiments. *P<0.05 vs. control. (A and B) The treatment of endothelial progenitor cells (EPCs) with BaP (20 μM) significantly increased the mRNA levels of the p65 and p50 subunits of NF-κB. (C) As shown by immunofluorescence staining, treatment with BaP induced NF-κB translocation. In the untreated cells, most of the staining for NF-κB was observed in the cytoplasm, while in the cells treated with BaP, staining significantly increased in the nucleus, suggesting that NF-κB translocated from the cytoplasm into the nucleus.

form capillary-like structures, EPCs were seeded on Matrigel® for 24 h after they were treated with BaP. BaP induced significant decreases in the number of capillary-like structures in a dose-dependent manner (Fig. 2D).

BaP increases oxidative stress in EPCs. To determine whether oxidative stress is involved in the action of BaP, ROS levels were analyzed. The treatment of EPCs with BaP (20 μM) for 45 min significantly increased cellular ROS levels, as indicated by the gray value of green fluorescence (Fig. 3A-D). Furthermore, BaP increased the production of MDA and suppressed the production of SOD (Fig. 3E and F). These data demonstrate that BaP increases oxidative stress in EPCs.

BaP increases NF-κB activity. BaP was then examined for its effect on NF-κB transcription and translocation. RT-PCR demonstrated that the treatment of EPCs with BaP (20 μM) significantly increased the mRNA levels of the p65 and p50 subunits of NF-κB (Fig. 4A and B). The morphological changes of NF-κB translocation indicated by immunofluorescence staining (Fig. 4C) showed that BaP induced NF-κB translocation. When the cells were left untreated, most of the

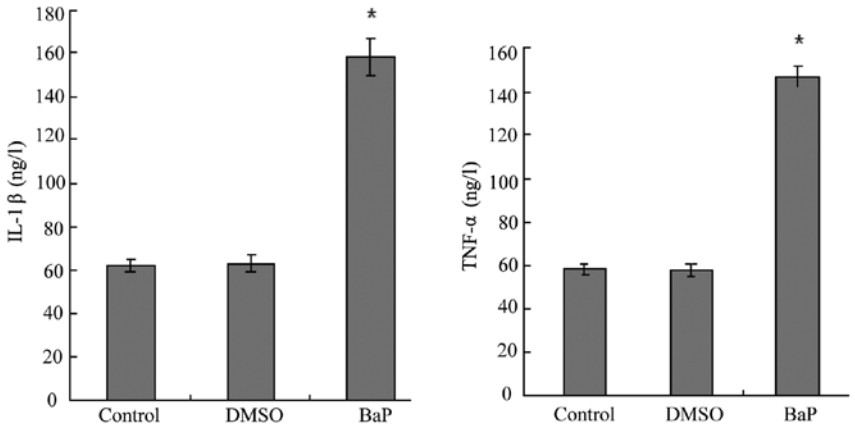

Figure 5. BaP induces the production of the pro-inflammatory cytokines, iterleukin (IL)-1β and tumor necrosis factor (TNF)-α, by endothelial progenitor cells (EPCs). Data represent the means ± SEM of at least 3 independent experiments. *P<0.05 vs. control.

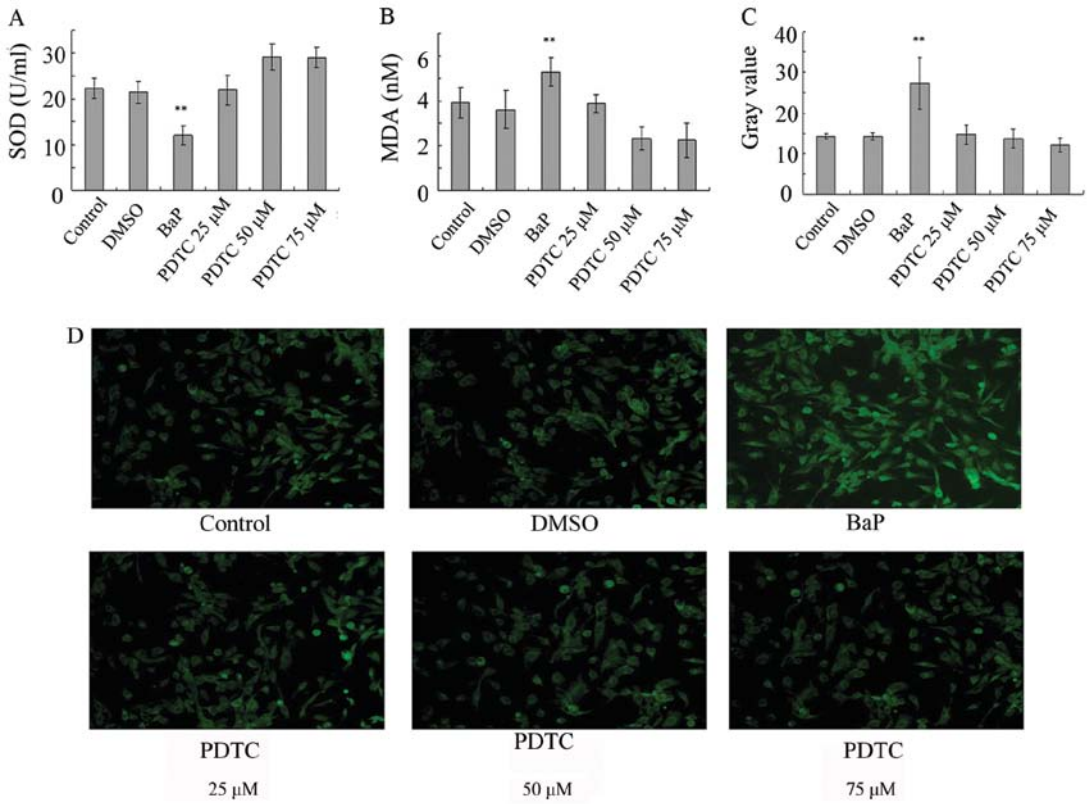

Figure 6. BaP-induced oxidative stress of endothelial progenitor cells (EPCs) is abolished by pyrrolidine dithiocarbamate (PDTC). Pre-treatment of EPCs with PDTC prior to BaP treatment significantly reversed superoxide dismutase (SOD) inhibition (A), and decreased the BaP-induced production of (B) malondialdehyde (MDA) and (C) ROS. (D) Representative fluorescence images demonstrating ROS production in each group. Data represent the means ± SEM of at least 3 independent experiments. **P<0.01 vs. control.

fluorescence staining for NF-κB was in the cytoplasm and rare NF-κB staining was observed in the nucleus. When the cells were stimulated with BaP, NF-κB staining significantly increased in the nucleus, suggesting that NF-κB translocated from the cytoplasm into the nucleus.

BaP increases the production of IL-1β and TNF-α. IL-1β and TNF-α are downstream targets of NF-κB. We then examined the effects of BaP on the production of IL-1β and TNF-α by EPCs. The results of ELISA for EPC culture supernatants showed that BaP (20 μM) increased the secretion of IL-1β and TNF-α by EPCs (Fig. 5).

Effects of BaP on EPCs are abolished by PDTC. As shown above, BaP significantly promoted NF-κB activation, increased intracellular ROS production and inhibited the proliferation, migration, adhesion and angiogenesis of EPCs *in vitro* in a dose-dependent manner. To evaluate the role of NF-κB, the effects of PDTC, a NF-κB inhibitor, on BaP-induced EPC dysfunction were examined. The pre-treatment of EPCs with PDTC prior

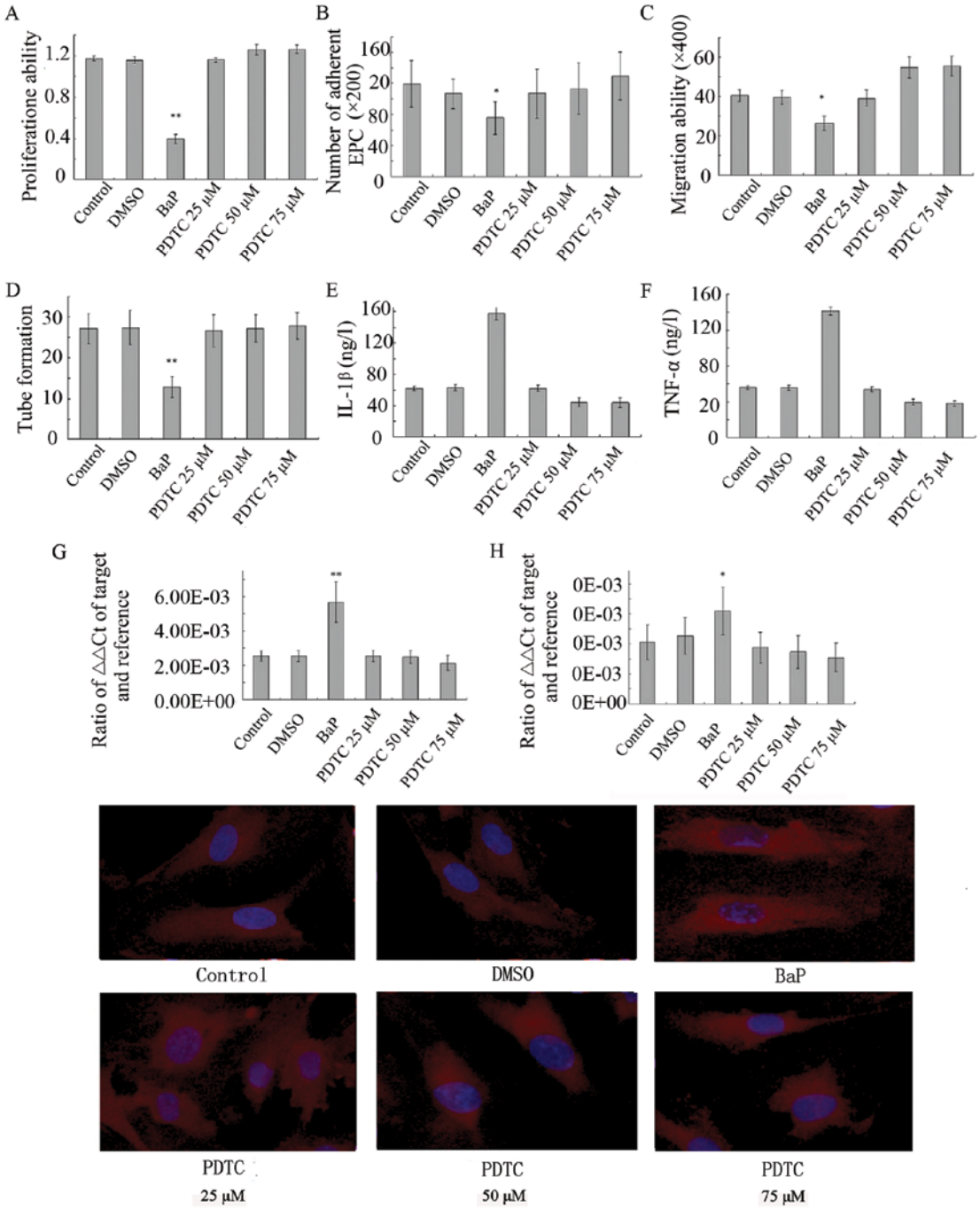

Figure 7. BaP-induced endothelial progenitor cell (EPC) dysfunction is abolished by pyrrolidine dithiocarbamate (PDTC). Pre-treatment of EPCs with PDTC prior to BaP treatment significantly reversed BaP-induced inhibition of (A) proliferation, (B) adhesion, (C) migration and (D) angiogenesis of EPCs. The BaP-induced production of (E) interleukin (IL)-1β and (F) tumor necrosis factor (TNF)-α and (G-H) activation of NF-κB were also prevented. (D) Representative images of NF-κB allocation. Data represent the means ± SEM of at least 3 independent experiments. *P<0.05 vs. control; **P<0.01 vs. control.

to BaP treatment significantly inhibited the stimulatory effect of BaP on oxidative stress (Fig. 6) and reversed BaP-induced EPC dysfunction in a dose-dependent manner (Fig. 7). These results suggest that BaP stimulates oxidative stress, at least in part, through the activation of NF-κB.

Discussion

To our knowledge, our study demonstrates for the first time that BaP hampers the function of EPCs. The major findings of our study are that BaP: i) inhibits EPC proliferation; ii) BaP modulates angiogenic-related properties of EPCs *in vitro*; iii) BaP increases oxidative stress in EPCs and iv) inhibits EPC proliferation at least in part, through the NF-κB pathway. Taken together, these findings provide a novel mechanism underlying the detrimental effects of BaP on vascular function, as EPCs play a critical role in angiogenesis and potentially aid in the repair of the injured endothelium (24-28).

A number of studies have shown that EPCs form a heterogenous population of cells. The most widely accepted phenotype for the identification of EPCs by FACS comprises $CD34^{+}$/kinase insert domain containing receptor $(KDR)^{+}$ and $CD133^{+}$/

KDR$^+$ cells (29-31). Bone marrow-derived EPCs possess the capacity to proliferate, migrate and differentiate into endothelial lineage cells (32). EPCs are mobilized from bone marrow into the circulation during vascular injury, and then home to the site of neovascularization and thereby contribute to postnatal neovascularization (33,34). Moreover, the findings that decreased levels of EPCs correlate with subsequent increases in cardiovascular events suggest that EPCs are important predictors of cardiovascular mortality and morbidity (15,35). Indeed, the number of circulating EPCs and their function have been reported to be reduced in patients with coronary artery disease (36), diabetes (37), metabolic syndrome (38) and severe heart failure (39).

Excessive generation of ROS and reactive nitrogen species may contribute to endothelial dysfunction and plays a critical role in the progressive deterioration of vessel structure and function (40). While low levels of ROS are essential and participate in important intracellular signaling pathways (41), excessive generation of ROS may result in cytotoxic oxidative stress. Cigarette smoke contains high concentrations of ROS, nitric oxide, peroxynitrite and free radicals of organic compounds (42,43). In addition to these short-lived, highly reactive substances, previous studies have shown that aqueous cigarette tar extracts also contain pro-oxidant substances that have the potential to increase the cellular production of ROS (44). It has thus been hypothesized that water-soluble components of cigarette smoke that are likely to reach the systemic circulation can directly promote oxidative stress in the vasculature and blood cells (42).

NF-κB is a ubiquitous nuclear transcription factor that plays a major regulatory role in inflammation. It resides in the inactive state in the cytoplasm as a heterotrimer consisting of p50, p65 and IκBα subunits. This transcription factor is a dimeric complex composed of different members of the Rel/NF-κB family of polypeptides. The p50-p65 heterodimer is retained in the cytoplasm by the inhibitory subunit, IκBα. Upon activation of the complex, IκBα sequentially undergoes phosphorylation, ubiquitination and degradation, thus releasing the p50-p65 heterodimer for translocation to the nucleus. An IκBα kinase, IKK, has been identified that phosphorylates serine residues in IκBα at position 32 and 36. The treatment of cells with various inflammatory and oxidative stress stimuli activates IKK, thus leading to the degradation of IκBα and activation of the transcription factor. Experimental data support the activation of the transcription factor NF-κB as a key redox-sensitive event associated with vascular dysfunction (45). The results of this study also demonstrate that the activation of NF-κB in EPCs is associated with a functional consequence, i.e., the decrease in the proliferation, migration and adhesion of EPCs. To further investigate the pro-inflammatory effect of BaP on EPCs, we examined the expression of NF-κB target genes (IL-1β and TNF-α). IL-1β and TNF-α were upregulated by BaP, and pre-treatment with NF-κB inhibitors diminished this overexpression, suggesting an NF-κB-mediated transcriptional mechanism.

In conclusion, the results of this study show that in cultured EPCs, BaP activates the NF-κB pathway, upregulating the expression of pro-inflammatory cytokines involved in atherosclerosis. This means that water-soluble components of cigarette smoke can promote oxidative stress not only of endothelial cells but possibly also of EPCs. This study also revealed that NF-κB p65 participates in the negative regulation of the oxidative stress of EPCs, and may provide a new insight into the possible role of NF-κB in suppressing EPC function. This pathway may be a novel therapeutic target in atherosclerosis. Further studies are required to confirm whether its inhibition is useful in the treatment of this disorder.

Acknowledgements

This study was supported by grants from the Zhenjiang Province Natural Science Foundation (no. Y2110550), the Research Project of Wenzhou Science and the Technology Bureau (nos. H20100056 and H20080027).

References

1. World Health Organisation Tobacco Free Initiative. Oslo, Norway: WHO Workshop on Advancing Knowledge on Regulating Tobacco Products, February 2000.
2. Rogot E and Murray JL: Smoking and causes of death among U.S. veterans: 16 years of observation. Public Health Rep 95: 213-222, 1980.
3. Howard G, Wagenknecht LE, Burke GL, *et al*: Cigarette smoking and progression of atherosclerosis: The Atherosclerosis Risk in Communities (ARIC) Study. JAMA 279: 119-124, 1998.
4. Jiang CQ, Xu L, Lam TH, Lin JM, Cheng KK and Thomas GN: Smoking cessation and carotid atherosclerosis: the Guangzhou Biobank Cohort Study-CVD. J Epidemiol Community Health 64: 1004-1009, 2010.
5. Rodgman A, Smith CJ and Perfetti TA: The composition of cigarette smoke: a retrospective, with emphasis on polycyclic components. Hum Exp Toxicol 19: 573-595, 2000.
6. Baird WM, Hooven LA and Mahadevan B: Carcinogenic polycyclic aromatic hydrocarbon-DNA adducts and mechanism of action. Environ Mol Mutagen 45: 106-114, 2005.
7. Shi Z, Dragin N, Miller ML, *et al*: Oral benzo[a]pyrene-induced cancer: two distinct types in different target organs depend on the mouse Cyp1 genotype. Int J Cancer 127: 2334-2350, 2010.
8. Griendling KK, Sorescu D and Ushio-Fukai M: NAD(P)H oxidase: role in cardiovascular biology and disease. Circ Res 86: 494-501, 2000.
9. Ross R: Atherosclerosis is an inflammatory disease. Am Heart J 138: S419-S420, 1999.
10. Libby P: Inflammation in atherosclerosis. Nature 420: 868-874, 2002.
11. Li DW, Liu ZQ, Wei J, Liu Y and Hu LS: Contribution of endothelial progenitor cells to neovascularization (Review). Int J Mol Med 30: 1000-1006, 2012.
12. Rabelink TJ, de Boer HC, de Koning EJ and van Zonneveld AJ: Endothelial progenitor cells: more than an inflammatory response? Arterioscler Thromb Vasc Biol 24: 834-838, 2004.
13. Hristov M, Zernecke A, Bidzhekov K, *et al*: Importance of CXC chemokine receptor 2 in the homing of human peripheral blood endothelial progenitor cells to sites of arterial injury. Circ Res 100: 590-597, 2007.
14. Hutter R, Carrick FE, Valdiviezo C, *et al*: Vascular endothelial growth factor regulates reendothelialization and neointima formation in a mouse model of arterial injury. Circulation 110: 2430-2435, 2004.
15. Hill JM, Zalos G, Halcox JP, *et al*: Circulating endothelial progenitor cells, vascular function, and cardiovascular risk. N Engl J Med 348: 593-600, 2003.
16. Ramos KS, Zhang Y, Sadhu DN and Chapkin RS: The induction of proliferative smooth muscle cell phenotypes by benzo[a] pyrene is characterized by up-regulation of inositol phospholipid metabolism and c-Ha-ras gene expression. Arch Biochem Biophys 332: 213-222, 1996.
17. Curfs DM, Lutgens E, Gijbels MJ, Kockx MM, Daemen M, and van Schooten FJ: Chronic exposure to the carcinogenic compound benzo[a]pyrene induces larger and phenotypically different atherosclerotic plaques in ApoE-knockout mice. Am J Pathol 164: 101-108, 2004.

18. Smaniotto S, Martins-Neto AA, Dardenne M and Savino W: Growth hormone is a modulator of lymphocyte migration. Neuroimmunomodulation 18: 309-313, 2011.
19. Kleinman HK and Martin GR: Matrigel: basement membrane matrix with biological activity. Semin Cancer Biol 15: 378-386, 2005.
20. Cominacini L, Garbin U, Pasini AF, *et al*: Oxidized low-density lipoprotein increases the production of intracellular reactive oxygen species in endothelial cells: inhibitory effect of lacidipine. J Hypertens 16: 1913-1919, 1998.
21. Heid CA, Stevens J, Livak KJ and Williams PM: Real time quantitative PCR. Genome Res 6: 986-994, 1996.
22. Gibson UE, Heid CA and Williams PM: A novel method for real time quantitative RT-PCR. Genome Res 6: 995-1001, 1996.
23. Ziegler-Heitbrock HW, Sternsdorf T, Liese J, *et al*: Pyrrolidine dithiocarbamate inhibits NF-kappa B mobilization and TNF production in human monocytes. J Immunol 151: 6986-6993, 1993.
24. Kalka C, Masuda H, Takahashi T, *et al*: Transplantation of ex vivo expanded endothelial progenitor cells for therapeutic neovascularization. Proc Natl Acad Sci USA 97: 3422-3427, 2000.
25. Hur J, Yoon CH, Kim HS, *et al*: Characterization of two types of endothelial progenitor cells and their different contributions to neovasculogenesis. Arterioscler Thromb Vasc Biol 24: 288-293, 2004.
26. Grunewald M, Avraham I, Dor Y, *et al*: VEGF-induced adult neovascularization: recruitment, retention, and role of accessory cells. Cell 124: 175-189, 2006.
27. Yamahara K and Itoh H: Potential use of endothelial progenitor cells for regeneration of the vasculature. Ther Adv Cardiovasc Dis 3: 17-27, 2009.
28. Sirker AA, Astroulakis ZM and Hill JM: Vascular progenitor cells and translational research: the role of endothelial and smooth muscle progenitor cells in endogenous arterial remodelling in the adult. Clin Sci 116: 283-299, 2009.
29. Peichev M, Naiyer AJ, Pereira D, *et al*: Expression of VEGFR-2 and AC133 by circulating human CD34(+) cells identifies a population of functional endothelial precursors. Blood 95: 952-958, 2000.
30. Urbich C and Dimmeler S: Endothelial progenitor cells: characterization and role in vascular biology. Circ Res 95: 343-353, 2004.
31. Salvatore P, Casamassimi A, Sommese L, *et al*: Detrimental effects of *Bartonella henselae* are counteracted by L-arginine and nitric oxide in human endothelial progenitor cells. Proc Natl Acad Sci USA 105: 9427-9432, 2008.
32. Asahara T and Kawamoto A: Endothelial progenitor cells for postnatal vasculogenesis. Am J Physiol Cell Physiol 287: C572-C579, 2004.
33. Kamihata H, Matsubara H, Nishiue T, *et al*: Implantation of bone marrow mononuclear cells into ischemic myocardium enhances collateral perfusion and regional function via side supply of angioblasts, angiogenic ligands, and cytokines. Circulation 104: 1046-1052, 2001.
34. Szmitko PE, Fedak PW, Weisel RD, Stewart DJ, Kutryk MJ and Verma S: Endothelial progenitor cells: new hope for a broken heart. Circulation 107: 3093-3100, 2003.
35. Werner N, Kosiol S, Schiegl T, *et al*: Circulating endothelial progenitor cells and cardiovascular outcomes. N Engl J Med 353: 999-1007, 2005.
36. Vasa M, Fichtlscherer S, Aicher A, *et al*: Number and migratory activity of circulating endothelial progenitor cells inversely correlate with risk factors for coronary artery disease. Circ Res 89: E1-E7, 2001.
37. Tepper OM, Galiano RD, Capla JM, *et al*: Human endothelial progenitor cells from type II diabetics exhibit impaired proliferation, adhesion, and incorporation into vascular structures. Circulation 106: 2781-2786, 2002.
38. Fadini GP, De Kreutzenberg SV, Coracina A, *et al*: Circulating $CD34^+$ cells, metabolic syndrome, and cardiovascular risk. Eur Heart J 27: 2247-2255, 2006.
39. Heeschen C, Lehmann R, Honold J, *et al*: Profoundly reduced neovascularization capacity of bone marrow mononuclear cells derived from patients with chronic ischemic heart disease. Circulation 109: 1615-1622, 2004.
40. Cai H and Harrison DG: Endothelial dysfunction in cardiovascular diseases: the role of oxidant stress. Circ Res 87: 840-844, 2000.
41. Sundaresan M, Yu ZX, Ferrans VJ, Irani K and Finkel T: Requirement for generation of H_2O_2 for platelet-derived growth factor signal transduction. Science 270: 296-299, 1995.
42. Pryor WA, Prier DG and Church DF: Electron-spin resonance study of mainstream and sidestream cigarette smoke: nature of the free radicals in gas-phase smoke and in cigarette tar. Environ Health Perspect 47: 345-355, 1983.
43. Pryor WA, Stone K, Zang LY and Bermudez E: Fractionation of aqueous cigarette tar extracts: fractions that contain the tar radical cause DNA damage. Chem Res Toxicol 11: 441-448, 1998.
44. Zang LY, Stone K and Pryor WA: Detection of free radicals in aqueous extracts of cigarette tar by electron spin resonance. Free Radic Biol Med 19: 161-167, 1995.
45. Haddad JJ: Oxygen sensing and oxidant/redox-related pathways. Biochem Biophys Res Commun 316: 969-977, 2004.